Optical properties of a CaF_2 crystal

Fanqi Gan, Yong-Nian Xu, Ming-Zhu Huang, and W. Y. Ching
Department of Physics, University of Missouri—Kansas City, Kansas City, Missouri 64110

Joseph G. Harrison
Department of Physics, University of Alabama at Birmingham, Birmingham, Alabama 35294
(Received 9 July 1991; revised manuscript received 4 November 1991)

The electronic structure, the charge-density distribution, and the optical-absorption spectrum of a CaF_2 crystal are studied by means of a first-principles local-density calculation. The calculated imaginary part of the dielectric function is in good agreement with experimental measurement up to 27.0 eV. We have also used a simplified self-interaction-correction (SIC) model to address the problem of band-gap underestimation in the local-density calculation. Although some marginal improvement in the optical result has been achieved, there is no strong evidence of unequivocal rectification other than an increment in the band gap. This study shows additional (non-SIC) correction to the conduction-band states of CaF_2 may also be necessary.

I. INTRODUCTION

CaF_2 is a representative alkaline earth fluoride that has been the subject of experimental and theoretical studies for years.[1-5] It is a highly ionic insulator with a large band gap. In addition to the usual energy-band structure, we were also interested in the calculation of its optical properties including $\epsilon_2(\omega)$. This was motivated in part by the optical measurements recently published by Barth, Johnson, and Cardona (BJC),[6] and also in part by a desire to further test the accuracy of the first-principles orthogonalized linear combination of atomic orbitals (OLCAO) method in the local-density approximation (LDA). Furthermore, we also wanted to test the effectiveness of using a simplified self-interaction-correction (SIC) model to improve the results of the LDA calculation.

The paper is organized as follows: We first briefly discuss the calculation method in Sec. II. That is followed by the presentation of calculated results for the band structure, density of states (DOS), effective ionic charge and optical properties of CaF_2 in Sec. III. In Sec. IV, we introduce our simplified SIC model and discuss the results obtained from such a model. Some concluding remarks are made in the last section.

II. METHOD OF CALCULATION

Our calculation has utilized the first-principles self-consistent OLCAO method. This method has been extensively applied to study the electronic and optical properties of a number of insulators.[7-11] As this method has been described in detail elsewhere,[7] we will only outline the major steps here. In the crystal calculation, the one-electron Schrödinger equation is solved self-consistently within the LDA approximation. The basis functions are expanded in terms of Bloch sums constructed from the atomic orbitals of F $(1s,2s,2p_x,2p_y,2p_z,3s,3p_x,3p_y,3p_z)$ and Ca $(1s,2s,2p_x,2p_y,2p_z,3s,3p_x,3p_y,3p_z,4s,4p_x,4p_y,4p_z,\ 3d_{xy},3d_{xz},3d_{yz},3d_{x^2-y^2},3d_{3z^2-r^2},5s,5p_x,5p_y,5p_z)$. The atomic orbitals are expressed as linear combinations of Gaussian-type orbitals (GTO). This basis set is generally referred to as a full basis because it consists of all the valence-shell orbitals plus another shell of empty orbitals. We have adopted the orthogonalization to the core procedure, which makes the computations more affordable. In the present work, the valence levels were taken as the F $2s$ and $2p$ bands because of their positions relative to the highest occupied Ca $2p$ band. In the self-consistent calculation, the accuracy of the charge-density fitting required in each iterative step is monitored by calculating the unconstrained integrated charge from the fitting functions and comparing it with total charge in the crystal. In our scheme, there are 16 valence electrons in a CaF_2 unit cell and our integrated charge is 16.000 17 electrons, which is indicative of the overall self-consistent-field (SCF) accuracy. After the self-consistency in the potential has been obtained, the eigenvalues and the eigenvectors of the band secular equations are solved at 505 $\mathbf{k}$ points in an irreducible portion of the Brillouin zone. The energies and wave functions at these $\mathbf{k}$ points are used to evaluate the DOS and optical conductivities using the linear analytic tetrahedron method.[12]

III. RESULTS OF CALCULATION

A. Band structure and density of states

The calculated band structure and DOS for CaF_2 are shown in Figs. 1 and 2, respectively. The lowest conduction-band (CB) state is at Γ, but the top of the valence-band (VB) states is at X. This indirect band gap of only 6.53 eV is much smaller than the experimental band gap of 12.1 eV.[2] Heaton and Lin (HL) obtained a band-gap value of 9.8 eV (indirect) by using a full Slater exchange in their self-consistent LCAO calculation.[1] It is well known that the use of full Slater exchange results in

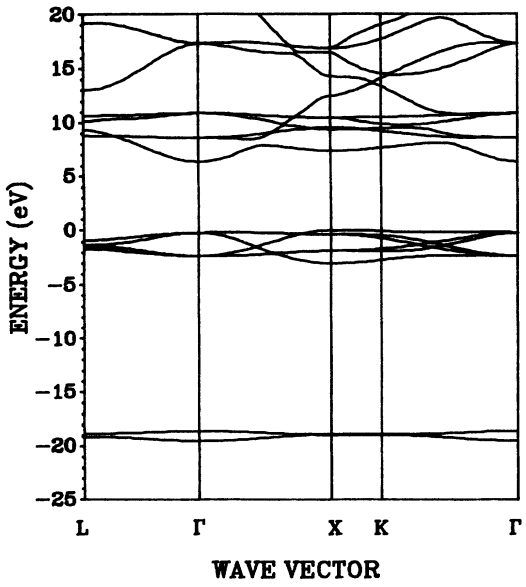

FIG. 1. Calculated band structure of CaF_2.

larger band gaps than the Kohn-Sham exchange in the usual LDA. HL had argued that the experimental value of 12.1 eV assigned by Rubloff[2] was too large. The recent work of BJC (Ref. 6) suggests a *direct* band gap of 11.6 eV. Albert, Jouanin, and Cout had also reported some band-structure results on CaF_2.[3,4] They used the LCAO method for the VB and the orthogonalized-plane-wave method for the CB. They used an overlapping-atomic-potential model and chose an exchange parameter of $\alpha=0.795$ in order to match the experimental band-gap value, while the full Slater exchange parameter $\alpha=1$ gave too large a gap.

In our calculation, the upper VB has two peaks centered at -2.5 and -0.5 eV, respectively. The total width of the upper VB is about 3.1 eV, which is in good agreement with the experimental value.[5] Other calculations gave somewhat narrower VB widths [2.0 eV by HL (Ref. 1) and 2.7 eV by Albert, Jouanin, and Cout[4]]. The lowest F 2*s* band is 1.1 eV wide and peaks at about -20.0 eV. The CB structure is more complicated, exhibiting five major peaks at 8.0, 9.0, 9.5, 10.0, and 10.5 eV.

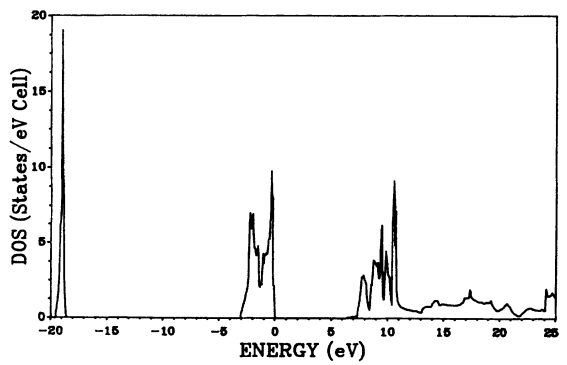

FIG. 2. Calculated DOS of CaF_2.

These peaks are very close to each other and there are more small structures at still higher energies.

B. Charge distribution

The valence charge-density distribution in an ionic crystal is an important part of the electronic structure. It relates directly to the effective ionic charge, a parameter which plays a major role in ionic conductivity. The accuracy of the electron charge distribution is also intimately connected to the accuracy of the calculated electronic contributions to the optical properties. In the empirical type of studies, the ions in CaF_2 are normally assumed to take on their canonical values of Ca^{2+} and F^-. In an LCAO-type calculation, it is traditional to use the Mulliken population scheme to estimate the effective charge on each ion. However, this method has its limitations because it works well only for systems in which atomic basis functions are not too diffuse. In our calculation we have used a full basis, which includes diffuse orbitals, in order to capture some of the features of the excited states of Ca and F, and to better represent the polarizability of the ions. Thus the conventional Mulliken scheme could give misleading results because of the large overlap of these extended orbitals. A much more reliable way to estimate the effective charge on each ion is by real-space integration of the self-consistent charge densities. In our method, the charge density of the crystal is decomposed into a lattice sum of atom-centered spherical Gaussians of varying decay exponents. An effective ionic charge can be determined by radially integrating the charge density up to an ionic radius which is determined from the inspection of a charge-density plot along an internuclear axis or from inspection of a two-dimensional contour plot. The charge density for CaF_2 along a Ca-F bond and in the [110] plane are shown in Figs. 3(a) and 3(b), respec-

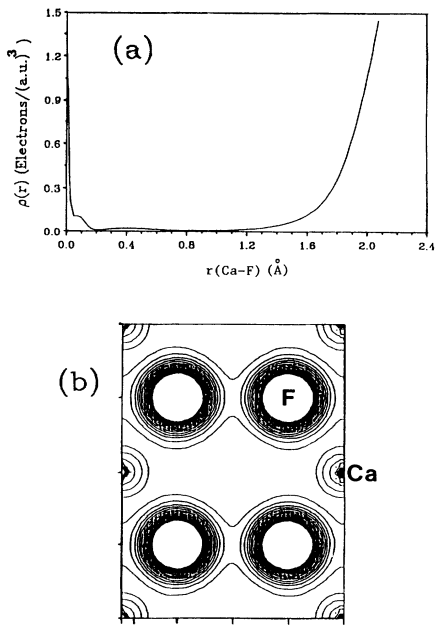

FIG. 3. Calculated charge density distribution in CaF_2: (a) along a Ca-F bond; (b) in the [110] plane.

tively. From these diagrams, we determine the effective ionic radius for Ca^{2+} and F^- ions to be 0.57 and 2.60 Å, respectively. In this way, we can divide the CaF_2 crystal into three regions: (a) the Ca sphere which accounts for 2.82% of the unit cell volume and contains only 0.04 electrons; (b) the two F spheres which account for 26.81% of the volume and contain 7.64 electrons in each sphere; (c) the interstitial region which accounts for the remaining 43.56% of the volume and contains 0.68 electron. If we divide the charges in the interstitial region among Ca and F in proportion to their effective volumes, we arrive at an ionic formula of $Ca^{1.95+}$ $F_2^{0.975-}$. This indicates that Ca and F each takes on formal charges close to the canonical values, indicative of the highly ionic nature of CaF_2.

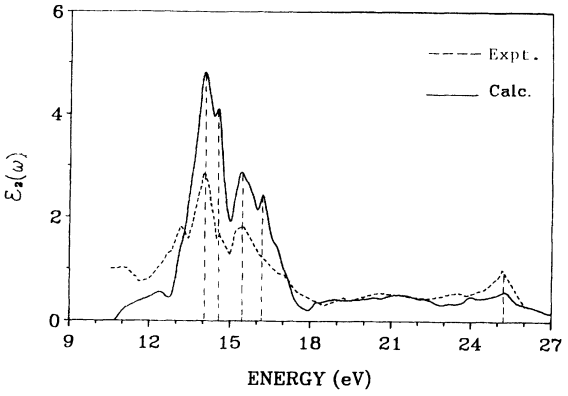

FIG. 4. Imaginary part of the dielectric function, $\epsilon_2(\omega)$, for CaF_2. The solid line represents the theoretical calculation; the dashed line represents the experimental curve from Ref. 6.

C. Optical properties

The calculation of the optical properties of CaF_2 is the major thrust of this paper. There is a long history of optical measurements on CaF_2 (Refs. 2, 5, and 13–16) and there are different and sometimes conflicting viewpoints in the interpretation of these experiments. Recently, BJC (Ref. 6) have undertaken a study of the optical properties of CaF_2. They used a newly developed vacuum ultraviolet (vuv) ellipsometer to determine the dielectric function of CaF_2. We believe that their result is more accurate than most of the previous investigations and therefore can be used to test the accuracy of the calculations.

In the first-principles OLCAO approach, the procedure to calculate the optical properties may be outlined as follows. The real part of the interband optical conductivity σ_I is calculated in the random-phase approximation using the Kubo-Greenwood formula:[17]

$$\sigma_I(E)=(e^2/4\pi^2 mE\Omega)\int d\mathbf{k}\sum_{n,l}|\langle\psi_n(\mathbf{k},\mathbf{r})|-i\hbar\nabla|\psi_l(\mathbf{k},\mathbf{r})\rangle|^2 f_l(\mathbf{k})[1-f_n(\mathbf{k})]\delta(E_n(\mathbf{k})-E_l(\mathbf{k})-E)\ , \tag{1}$$

where $E=\hbar\omega$ is the photon energy, Ω is the unit-cell volume, and $f(\mathbf{k})$ is the Fermi distribution function. The band index l indicates an occupied state and n an empty state. The momentum matrix elements $\langle\psi_n(\mathbf{k},\mathbf{r})|-i\hbar\nabla|\psi_l(\mathbf{k},\mathbf{r})\rangle$ in Eq. (1) are calculated from the crystal wave functions at each $\mathbf{k}$ point. The imaginary part of the linear dielectric function is obtained from $\sigma_I(\omega)$ as

$$\epsilon_2(\omega)=(4\pi/\omega)\sigma_I(\omega)\ , \tag{2}$$

while the real part can be obtained from $\epsilon_2(\omega)$ by a Kramers-Kronig transformation.

One of the important optical constants is the static dielectric constants ϵ_0, or $\epsilon_1(0)$. Since the measured $\epsilon_1(\omega)$ in the low-frequency region may contain contributions from lattice vibrations, the calculated ϵ_0 value, which only accounts for the electronic contribution, is generally smaller than the measured value. With large-band-gap crystals, the lattice vibrational effects can be ignored in the frequency region around 2.0 eV.

In Fig. 4 we compare our calculated $\epsilon_2(\omega)$ with the measurement of BJC.[6] We have applied a shift of 4.2 eV in the energy scale for the calculated curve so as to align the major peak with the experimental one. This greatly simplifies the comparison of the structures in the absorption curves. We note that this shift is about 0.9 eV smaller than the difference of 5.07 eV between the calculated gap and the gap reported in Ref. 6. The calculated ϵ_0, 2.02, is larger than the extrapolated value of 1.50 for the experiment of Refs. 6 and 14 but is in good agreement with the value of 2.04 as given by Lines.[18] The calculated $\epsilon_2(\omega)$ shows five major peaks at 14.0, 14.6, 15.5, 16.2, and 25.2 eV. The same structures can be identified in the experimental curve. However, the calculated peak at 16.2 eV appears to be too strong. On the other hand, the well-defined experimental peak at 13.2 eV appears as a weak shoulder in the calculated curve. In general, it is fair to say that the experimental structures are well reproduced by the calculation, but the relative intensities of the structures are somewhat different. One reason for this discrepancy is that in our calculation, we have assumed the crystal to be at $T=0$ K and thus do not include vibronic contributions that are present in the room-temperature measurements. At higher frequency, vibronic contribution will be much less significant. This is consistent with the fact that the agreement between the calculated and measured curves is much more reasonable in the high-frequency region. There is some difference in the peak positions in the 28–35-eV region. Since the accuracy of the data at such a high energy will generally be somewhat degraded and may involve core excitations (not included in the present calculation), we think a precise understanding of structure at such a high-energy region requires further experimental as well as theoretical investigation.

IV. SELF-INTERACTION CORRECTION

It is well known that in covalently bonded semiconductors, the band gap predicted by the LDA theory is underestimated by as much as 30–40 %. There have been many approaches to overcome this shortcoming, ranging from the very simple "scissors operator" to the more sophisticated approaches such as the self-interaction correction[19] (SIC) and *GW* methods.[20–22] The scissors operator accounts for a rigid shift of all CB states by a fixed amount so as to match the accepted experimental value of the band gap. Surprisingly, the scissors operator works pretty well in many instances in spite of its simplicity. Perdew and Zunger[23,24] (PZ) have proposed a correction to the LDA, which in the context of energy-band theory leads to a modification of the band gap by removing the self-interaction error in an orbital-by-orbital fashion. Earlier work by Perdew[25] and Lindgren,[26] among others (see references in Ref. 23) demonstrated that when the self-Coulomb and an approximate self-exchange energy are subtracted from the total-energy functional, a remarkable improvement in the self-consistent-field solution for atoms and negative ions could be obtained. The SIC treatment subsequently has been applied to a variety of free atoms and to solids.[23,27–31] Later studies focused on developing practical schemes for the construction of the correction term for molecules and solids.[31,32] HL formulated SIC for the energy-band theory of crystals and applied it to LiCl and Ar band structures. They obtained very satisfactory results by generating Wannier-like orbital densities.[27,33,34] It should be noted that this correction for insulators is only applicable to the VB. Modification of the unoccupied (virtual) bands goes beyond SIC and has only been addressed parenthetically in the previously noted works. Application to metals has been addressed in the context of an electron-gas model.[35]

In a different approach, Louie and co-workers[20–22] have used the *GW* approximation to evaluate the self-energy operator in their first-principles theory of quasiparticle energies in semiconductors and insulators. The self-energy operator arises in the application of Green's-function techniques to the electron correlation problem.[36,37] The Green's-function approach permits a rigorous formulation of quasiparticle properties and thus address features associated with the CB states. They begin with the formulation of the one-particle excitation energies of an interacting system in a crystal potential:[36]

$$(\mathbf{T}+V_{\text{ext}}+V_c)\Psi_{nk}(\mathbf{r})+\int d\mathbf{r}'\Sigma(\mathbf{r},\mathbf{r};E_{nk})\Psi_{nk}(\mathbf{r}') = E_{nk}\Psi_{nk}(\mathbf{r}) , \quad (3)$$

where $\mathbf{T}$ is the kinetic energy operator, V_c is the Coulomb potential, V_{ext} is the external potential due to ions, Σ is the self-energy operator and it contains the effects of correlation and exchange among the electrons. In order to obtain the quasiparticle energies, it is necessary to evaluate Σ first and solve this equation. Hybertsen and Louie[20] used an expansion of the self-energy operator in terms of the dynamically screened Coulomb interaction (W) and the dressed Green's function (G) (hence the name of the *GW* method). Very good results were obtained using this approach. They concluded that the correction primarily applies to CB electrons in homopolar materials, such as diamond, Si, and Ge, but the correction is evenly divided between VB and CB for ionic crystals such as LiCl.[20] Although the *GW* results would seem to suggest that SIC could only capture half the correction needed for CaF_2, the correspondence between *GW* and orbital SIC may not be that simple. In this paper we follow the orbital SIC prescription and defer any discussion of its relationship to the *GW* correction.

A. The self-interaction error

In the Hartree-Fock theory, self-Coulomb and self-exchange terms are introduced to the one-particle equations to make the solutions more tractable without sacrificing constraints of physical reality because they exactly cancel one another. In the local-density theory, an approximate exchange-correlation term is introduced to solve the single-particle Schrödinger equation. Because of this approximation, the self-Coulomb interaction is only partially removed and the residual (nonphysical) self-interaction tends to shift the energy state upwards.[23,24] Because the VB states have a more localized charge distribution than the CB states, this upward shift in VB states is larger than that in the CB states, resulting in a reduction in the band gap. The CB states correspond more closely to electron affinity levels, because of their status as virtual-level solutions to an n-electron problem. Thus the error we should attribute to them is not what we would normally identify as a self-interaction error but rather a more traditional electron correlation error. In order to rectify the situation in regard to the occupied levels, a correction in potential, termed self-interaction correction, must be instituted in the electronic structure calculation.

In density-functional theory the total-energy functional can be expressed as

$$E_t = T_0 + V_{\text{ext}} + U_c + E_{\text{xc}} , \quad (4)$$

where T_0 is the noninteracting kinetic energy, V_{ext} is the external interaction, U_c is the Coulomb energy, and E_{xc} is the exchange-correlation energy. Since a point electron does not self-interact, we require an orbital-based density-functional description of electrons to satisfy

$$U_c[\rho_{i\sigma}]+E_{\text{xc}}[\rho_{i\sigma},0]=0 , \quad (5)$$

where $\rho_{i\sigma}$ is the orbital density for a single electron with spin index σ ($=\uparrow,\downarrow$). But in the LDA, the local approximation leads to an exchange-correlation correction term

$$E_{\text{xc}}=\int \rho_{i\sigma}(\mathbf{r})\epsilon_{\text{xc}}[\rho_{i\sigma}(\mathbf{r}),0)]d\mathbf{r} . \quad (6)$$

As a result,

$$U_c[\rho_{i\sigma}]+E_{\text{xc}}[\rho_{i\sigma},0]\neq 0 . \quad (7)$$

It is therefore necessary to introduce an extra term U_{sic} which satisfies

$$U_c[\rho_{i\sigma}]+E_{\text{xc}}[\rho_{i\sigma},0]+U_{\text{sic}}[\rho_{i\sigma}]=0 , \quad (8)$$

where $U_{\rm sic}$ is the term that will make the orbital-by-orbital correction. A universal prescription proposed by PZ (Ref. 23) for formulating this correction is

$$U_{\rm sic}=-\sum_{\sigma}\sum_{i}(E_{\rm xc}^{\rm LDA}[\rho_{i\sigma},0]+U_c[\rho_{i\sigma}]) , \tag{9a}$$

$$E_t^{\rm SIC\text{-}LDA}=E_t^{\rm LDA}+U_{\rm sic} . \tag{9b}$$

Because of the lack of transformation invariance, the formula derived by PZ poses some computational problems, especially in application to crystals. While Pederson, Heaton, and Lin[31] have removed the central difficulty by introducing a "canonical" set of SIC orbitals, it is still necessary to develop an efficient scheme for solving the self-consistent equations which follow from Eq. (9). As noted earlier, HL have presented a formulation for incorporation of SIC in the crystals.[19] In their work, the SIC to the total energy of the n-electron system is expressed in terms of Wannier functions. Excellent agreement was achieved for the band gap of LiCl between the SIC-LDA calculation and experiment.

B. Mulliken-weighted self-interaction correction

The procedures outlined by HL made application of SIC to crystalline solids possible. However, the scheme involves the construction of Wannier functions, which is quite complicated, especially when the crystal under study has a complex unit cell. It is desirable to have a simpler, yet effective SIC procedure to make the computation more practical. The model we adopt here is referred to as the Mulliken-weighted SIC method.[32]

In the ordinary (non-SIC) LDA energy-band calculations, we have

$$H^{\rm LDA}|\Psi_{nk}\rangle=\varepsilon_n(\mathbf{k})|\Psi_{nk}\rangle , \tag{10}$$

where $H^{\rm LDA}$ is the usual LDA Hamiltonian and Ψ_{nk} is the crystal wave function of the nth band with wave vector $\mathbf{k}$ which can be expressed as

$$|\Psi_{nk}\rangle=\sum_{\mu}\sum_{i}C_{in}^{\mu}(\mathbf{k})|b_{ik}^{\mu}\rangle , \tag{11}$$

where μ covers different atoms within a unit cell and the Bloch sum is given by

$$|b_{ik}^{\mu}\rangle=N^{-1/2}\sum_{\nu}\exp(i\mathbf{k}\cdot\mathbf{R}_{\nu})\Phi_i(\mathbf{r}-\mathbf{R}_{\nu}-\mathbf{t}_{\mu}) , \tag{12}$$

where i is the orbital index, $\mathbf{R}_{\nu}$ is the lattice translational vector, and Φ_i is an atom-centered linear combination of GTO (or single GTO to supplement the basis set). The solution of the SIC-LDA equations,

$$H^{\rm SIC\text{-}LDA}|\Psi_{nk}\rangle=\varepsilon_n(\mathbf{k})|\Psi_{nk}\rangle , \tag{13}$$

can be formulated in terms of LDA counterparts by adopting a Bloch-sum basis of M orbitals to reduce the problem to a linear eigensystem problem. It can be shown that the matrix form of the SIC-LDA Hamiltonian $H^{\rm SIC\text{-}LDA}$ takes the following form[32]

$$H^{\rm SIC\text{-}LDA}=H^{\rm LDA}-D^{\dagger}(K^0+A+A^{\dagger}-E)D+FD+D^{\dagger}F^{\dagger} , \tag{14}$$

where the matrices D, A, K^0, E, and F are constructed as follows:

$$D=C^{\dagger}S , \tag{15}$$

$$A=C^{\dagger}F , \tag{16}$$

$$K^0=C^{\dagger}H^{\rm LDA}C , \tag{17}$$

$$E_{ij}=(A_{ii}+K_{ii}^0)\delta_{ij} , \tag{18}$$

where S and C represent the LDA overlap matrix and eigenvectors, respectively, and a dagger designates Hermitian conjugation. The matrix F carries the SIC-related information in the form of matrix elements between Bloch sums and crystal wave functions:

$$(F^{\mu})_{\alpha n}=\langle b_{\alpha k}^{\mu}|\Delta V_{nk}|\Psi_{nk}\rangle , \tag{19}$$

where ΔV_{nk} is the $\mathbf{k}$-dependent SIC potential for the nth band as originally derived from the Wannier-function formulation by HL:[34]

$$\Delta V_{nk}=\sum_{\mu}\sum_{\nu}V_{n\mu}^{\rm SIC}(\mathbf{r}-\mathbf{R}_{\nu}-\mathbf{t}_{\mu})\exp(i\mathbf{k}\cdot\mathbf{R}_{\nu}) \times W_n^{\mu}(\mathbf{r}-\mathbf{R}_{\nu}-\mathbf{t}_{\mu})/\Psi_{nk} , \tag{20}$$

where $V_{n\mu}^{\rm SIC}(\mathbf{r}-\mathbf{R}_{\nu}-\mathbf{t}_{\mu})$ is the SIC potential pertaining to atom μ. As discussed above, the problem of constructing localized Wannier functions $W_n^{\mu}(\mathbf{r}-\mathbf{R}_{\nu}-\mathbf{t}_{\mu})$ can be quite difficult and subject to ambiguity related to phase choice. In our simplified model, we replace the Wannier function by the localized orbital:[27,34]

$$u_{nk}^{\mu}(\mathbf{r}-\mathbf{R}_{\nu}-\mathbf{t}_{\mu})=\sum_{l}C_{ln}^{\mu}(\mathbf{k})\Phi_l(\mathbf{r}-\mathbf{R}_{\nu}-\mathbf{t}_{\mu}) , \tag{21}$$

where l labels the atom-centered orbitals and simultaneously, replacing SIC potential by a Mulliken-weighted combination of orbital SIC potentials:

$$V_{n\mu}^{\rm SIC}=\sum_{l}\rho_{ln}^{\mu}(\mathbf{k})V_l^{\rm SIC} , \tag{22}$$

where $\rho_{ln}^{\mu}(\mathbf{k})$ is the Mulliken population of atomic orbital l of atom species μ for the state $n\mathbf{k}$. $V_l^{\rm SIC}$ is constructed

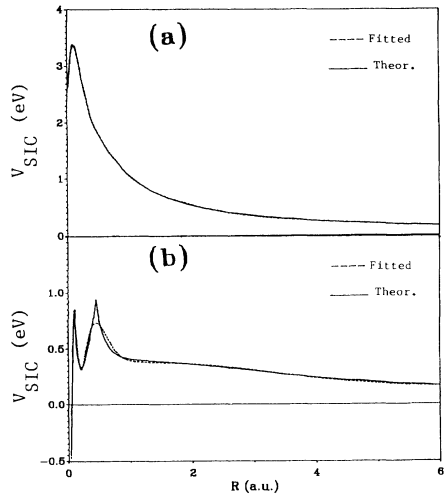

FIG. 5. (a) The F $2p$ orbital–SIC potential. (b) The Ca $3s$ orbital–SIC potential.

for each orbital of the atom (including the core orbital) by removing one electron in the orbital charge density for the usual V_{ext} in the LDA. V_l^{SIC} is then fitted nonlinearly to a sum of Gaussian functions to facilitate the evaluation of the matrix elements of V_l^{SIC} in Eq. (19). The numerically calculated and fitted V_l^{SIC} for F $2p$ and Ca $3s$ orbitals are shown in Figs. 5(a) and 5(b) as illustration. As we discussed above, Mulliken analysis is better suited to a minimal basis. So we use a minimal basis to perform the Mulliken analysis needed in the construction of Eq. (22), while retaining a full basis calculation in the final band structure and optical conductivity. After obtaining $V_{n\mu}^{SIC}$, we have then to calculate the matrix elements of the type

$$\langle b_{\alpha k}^{\mu}|\Delta V_{nk}|\Psi_{nk}\rangle = N^{-1/2}\sum_{\xi}\sum_{l} C_{ln}^{\xi}\sum_{\nu} e^{i\mathbf{k}\cdot\mathbf{R}_\nu}\langle b_{\alpha\mathbf{k}}^{\mu}|\Phi_l(\mathbf{r}-\mathbf{R}_\nu-\mathbf{t}_l)V_{n\xi}^{SIC}(\mathbf{r}-\mathbf{R}_\nu-\mathbf{t}_\xi)\rangle \tag{23}$$

in order to form the elements of the F matrix. By making use of the translational properties of the Bloch sum, Eq. (23) can be reduced to a summation over a series of two-center integrals.[34] With these matrices evaluated, we are then able to construct the Hamiltonian matrix as given in Eq. (14). Thus the solution of Eq. (13) can be reduced to the usual eigensystem problem encountered in LDA computations involving a finite basis set. The algebraic steps missing in the above discussion are taken up in Refs. 29, 32, and 34.

With the solution of Eq. (13), we obtain eigenvectors to construct a new Hamiltonian H^{LDA} and the new Mulliken populations needed to start an iterative procedure for SIC. This iteration is carried through several times until eigenvalues converge to a predetermine criterion. As one might expect, this SIC iterative procedure is carried out more efficiently if the SCF-LDA solution is used as a starting point, rather than incorporating SIC starting with the zeroth iteration of the self-consistent band calculation. The final eigenvalues and eigenvectors are used to evaluate the optical properties as discussed in Sec. III C.

C. Results with self-interaction correction

The SIC-LDA band structure is shown in Fig. 6. One obvious feature is the downward shift of the VB; the CB is only slightly changed. This is to be expected since there is no formal SIC correction for the CB and any shift comes about because of the slight change in the final LDA Hamiltonian as a result of the change in the SCF density because of the SIC. The shape of the energy-band structure remains the same except for a small decrease in the VB width (from 3.1 to 3.0 eV). Thus the band gap is enlarged from the original 6.35 eV to 8.20 eV. While this represents a substantial improvement, the value is still smaller than the experimental value of 11.6 eV by 3.4 eV (or 29%). It should be pointed out that in a finer energy scale, the shift in the VB in Fig. 6 as the result of SIC is nonuniform because the Mulliken weight has different components of SIC from different orbitals and different atoms at different $\mathbf{k}$ points.

The calculated imaginary part of the dielectric function after applying the simplified SIC is shown in Fig. 7. A 2.9-eV shift, which is 0.5 eV smaller than the gap underestimate, has been applied to align the major peak in the calculated curve and the measured curves. Comparing this with the LDA result of Fig. 4, there appear to be three areas of improvement. First, the intensity of the calculated curve is reduced and corresponds more closely to the experimental curve. Second, ϵ_0 is reduced to 1.80, in better agreement with the measured value. Third, the peak at 13.2 eV becomes more prominent. However, these improvements are offset by other increased discrepancies. For example, the peak at 14.6 eV, next to the most prominent peak, is not as visible in the experimental curve; and the intensity of the calculated curve above 18 eV is not as close to the experimental curve as the LDA result. Thus, on the whole, the improvement on the optical properties by SIC in CaF_2 is marginal at best, except for the marked improvement in enlarging the band gap.

In Fig. 8, we display the same calculation of $\epsilon_2(\omega)$ by applying the scissors operator which the CB was rigidly shifted by about 5.1 eV. In order to align the major peak in $\epsilon_2(\omega)$, a shift of 0.7 eV backward is necessary. The overall agreement with experiment is not improved over either the LDA or the LDA-SIC results. The main difference is that the intensity of spectra in this calculated curve is greatly reduced, and the peak at 13.2 eV appears to be even weaker by comparison to the LDA result. The ϵ_0 is reduced to 1.49, which is expected since the band

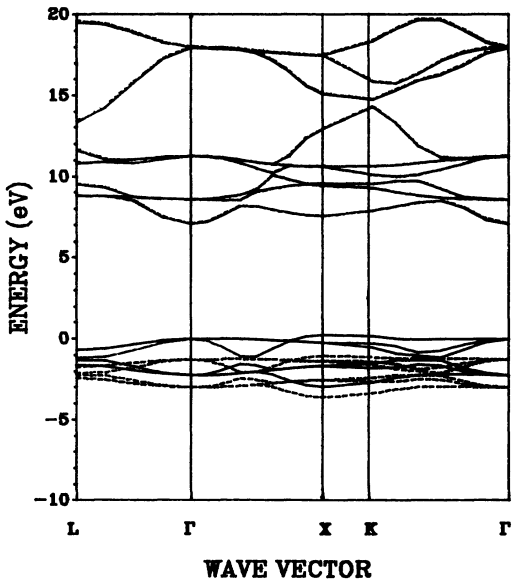

FIG. 6. Band structure of CaF_2: Solid line, without SIC; dashed line, with SIC. The zero of energy is set at the top of VB without SIC.

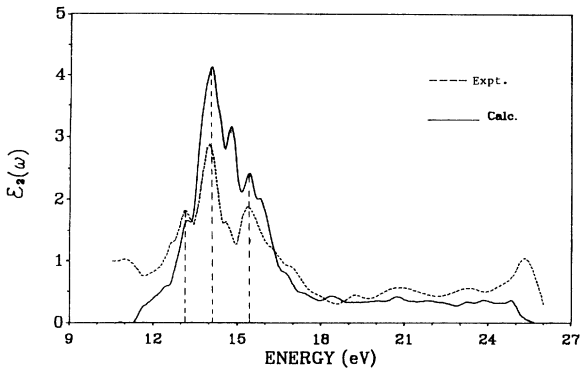

FIG. 7. Imaginary part of the dielectric function after inclusion of SIC. The solid line represents the theoretical calculation; the dashed line represents the experimental curve from Ref. 6.

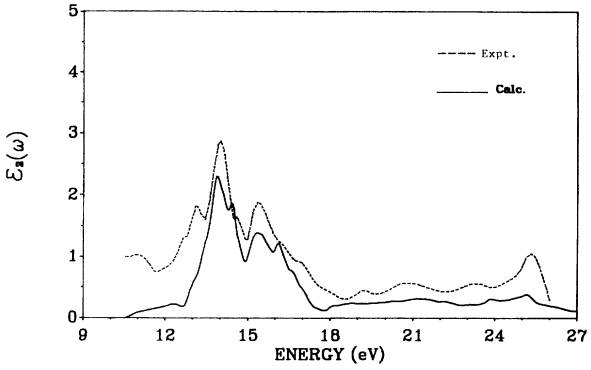

FIG. 8. Imaginary part of the dielectric function after applying the scissors operator. The solid line represents the theoretical calculation; the dashed line represents the experimental curve from Ref. 6.

gap has been greatly enlarged to match the experimental value. It is not clear that ϵ_0 and the intensity of the spectrum in the SIC calculation can be improved if further correction to the CB can be implemented.

V. CONCLUSION

We have presented results of our first-principles studies of the electronic structure and optical properties of CaF_2. A number of important physical parameters such as the bandwidth and band gap are obtained. A detailed analysis of charge distribution in CaF_2 based on direct-space integration shows the ionic formula to be $Ca^{1.95+}F_2^{0.975-}$. The calculated dielectric function for CaF_2 is in good agreement with a recent experimental measurement. A computationally efficient Mulliken-weighted SIC model was introduced in our band structure and optical calculation. The calculated band gap has been increased from 6.53 to 8.20 eV. However, the gap value after SIC is still underestimated by about 29% and the difference in the absorption intensity in the measured and calculated curves, while reduced, still remains. In a previous application of this method to an energy-band calculation of *trans*-polyacetylene (CH_x),[32] the calculated band gap was *larger* than experiment (3.6 eV compared to 1.8 eV). Also the SIC-LDA VB width was *increased* relative to the LDA value (17.6 eV compared to 16.8 eV). This is in contrast to the present result on CaF_2. One difference in the implementation of the Mulliken-weighted SIC in Ref. 32 and the present case is the use of an angular dependence in the atomic SIC potential [Eq. (22)] in Ref. 32. In the context of the CH_x system, which is characterized by distinct π and σ subbands in the VB, the preservation of the angular dependence in the p-orbital SIC potentials was imperative. In CaF_2, we do not believe it would be necessary to include such a modification due to the closed-shell nature of the ions involved. However, the unit-cell structure of CaF_2 suggests the possibility of developing a π- and σ-SIC correction which could further modify the VB width and position relative to the CB. It is also possible that a more rigorous Wannier function approach to SIC, or a different approach to the relative ordering of the iterative procedures in applying SIC and in the self-consistent LDA calculation may change the results somewhat. While these considerations *might* improve the calculated results to a certain extent, we cannot completely disregard the observation of Hybertsen and Louie[20] that the self-energy correction is evenly divided between VB and CB in the ionic crystal LiCl. This may suggest that further improvement will require more than a SIC correction. We may conclude that the self-interaction correction provides a substantial but not fully adequate improvement in the energy-band gap in CaF_2. Further correction to the CB may be necessary along the lines of Ref. 21 or in a formulation of a correction to the CB states in the spirit of the virtual-state Hamiltonian as discussed in Ref. 28. The optical properties calculated on the LDA theory give quite good result in agreement with experiment and probably will not be drastically changed by additional corrections.

ACKNOWLEDGMENT

This work was supported by the U.S. Department of Energy under Grant No. DE-FG02-84ER45170.

[1]R. A. Heaton and Chun C. Lin, Phys. Rev. B **22**, 3629 (1980).
[2]G. W. Rubloff, Phys. Rev. B **5**, 662 (1971).
[3]J. P. Albert, C. Jouanin, and C. Cout, Phys. Rev. B **16**, 4619 (1977).
[4]J. P. Albert, C. Jouanin, and C. Cout, Phys. Rev. B **16**, 925 (1977).
[5]R. T. Pool, J. Szajman, R. C. G. Leckey, J. G. Jenkin, and J. Liesegang, Phys. Rev. B **12**, 5872 (1975).
[6]J. Barth, R. L. Johnson, and M. Cardona, Phys. Rev. B **41**, 3291 (1990).
[7]W. Y. Ching, J. Am. Ceram. Soc. **73**, 3135 (1990).
[8]Y.-N. Xu and W. Y. Ching, Phys. Rev. B **43**, 4463 (1991); **44**, 7787 (1991).
[9]Y.-N. Xu and W. Y. Ching, Phys. Rev. B **41**, 5471 (1990).

[10]W. Y. Ching and Y.-N. Xu, Phys. Rev. Lett. **65**, 895 (1990); Phys. Rev. B **44**, 5332 (1991).
[11]Y.-N. Xu, W. Y. Ching, and R. H. French, Ferroelectrics **111**, 23 (1990); J. C. Parker, D. J. Lam, Y.-N. Xu, and W. Y. Ching, Phys. Rev. B **42**, 5289 (1990).
[12]G. Lehmann and M. Taut, Phys. Status Solidi **54**, 469 (1972); O. Jeksen and O. K. Andersen, Solid State Commun. **9**, 1763 (1971).
[13]T. Tomiki and T. Miyata, J. Phys. Soc. Jpn. **27**, 658 (1969).
[14]G. Stephan, Y. le Calvez, J. C. Lemonier, and S. Robin, J. Phys. Chem. Solids **30**, 601 (1969).
[15]W. Hayes, A. B. Kunz, and E. E. Koch, J. Phys. C **4**, L200 (1971).
[16]J. Frandon, B. Lahaye, and F. Pradal, Phys. Status Solidi B **53**, 565 (1972).
[17]D. Greenwood, Proc. Phys. Soc. London **71**, 585 (1958).
[18]M. E. Lines, Phys. Rev. B **41**, 3372 (1990).
[19]R. A. Heaton and Chun C. Lin, Phys. Rev. B **17**, 1853 (1984).
[20]M. S. Hybertsen and S. G. Louie, Phys. Rev. B **34**, 5390 (1986).
[21]M. S. Hybertsen and S. G. Louie, Phys. Rev. B **37**, 2733 (1988).
[22]M. P. Surh, S. G. Louie, and M. L. Cohen, Phys. Rev. B **43**, 9126 (1991).
[23]J. P. Perdew and A. Zunger, Phys. Rev. B **23**, 5048 (1981).
[24]A. Zunger, J. P. Perdew, and G. L. Oliver, Solid State Commun. **34**, 933 (1980).
[25]J. P. Perdew, Chem. Phys. Lett. **64**, 127 (1979).
[26]I. Lindgren, Int. J. Quantum Chem. Symp. **5**, 411 (1971).
[27]R. A. Heaton, J. G. Harrison, and C. C. Lion, Solid State Commun. **41**, 827 (1982).
[28]J. G. Harrison, R. A. Heaton, and C. C. Lin, J. Phys. B **16**, 2079 (1983).
[29]L. A. Cole and J. P. Perdew, Phys. Rev. A **25**, 1265 (1982).
[30]J. P. Perdew and M. R. Norman, Phys. Rev. B **26**, 5445 (1982).
[31]M. R. Pederson, R. A. Heaton, and C. C. Lin, J. Chem. Phys. **82**, 2688 (1985).
[32]J. G. Harrison, in *Density Functional Methods in Chemistry,* edited by J. K. Labanowski and J. W. Andzelm (Springer-Verlag, New York, 1991), Chap. 13.
[33]R. A. Heaton and C. C. Lin, Phys. Rev. B **25**, 3528 (1982).
[34]R. A. Heaton, J. G. Harrison, and C. C. Lin, Phys. Rev. B **28**, 5992 (1983).
[35]J. G. Harrison, Phys. Rev. B **35**, 987 (1987); M. R. Pederson, R. A. Heaton, and J. G. Harrison, *ibid.* **39**, 1581 (1989).
[36]L. Hedin and S. Lundqvist, in *Solid State Physics,* edited by H. Ehrenreich, F. Seitz, and D. Turnbull (Academic, New York, 1969), Vol. 23 p. 1.
[37]L. Hedin, Phys. Rev. **139**, A796 (1965).